Available online at www.sciencedirect.com
ScienceDirect
Journal of Hazardous Materials 155 (2008) 45–50
Journal of Hazardous Materials
www.elsevier.com/locate/jhazmat

Photocatalyzed degradation of flumequine by doped TiO_2 and simulated solar light

J. Nieto [a], J. Freer [b], D. Contreras [c], R.J. Candal [d], E.E. Sileo [d], H.D. Mansilla [a,*]

[a] *Departamento de Química Orgánica, Facultad de Ciencias Químicas, Universidad de Concepción, Casilla 160-C, Concepción, Chile*
[b] *Centro de Biotecnología, Facultad de Ciencias Químicas, Universidad de Concepción, Casilla 160-C, Concepción, Chile*
[c] *Departamento de Química Analítica e Inorgánica, Facultad de Ciencias Químicas, Universidad de Concepción, Casilla 160-C, Concepción, Chile*
[d] *INQUIMAE, Facultad de Ciencias Exactas y Naturales, Universidad de Buenos Aires, Argentina*

Received 4 July 2007; received in revised form 9 November 2007; accepted 12 November 2007
Available online 17 November 2007

Abstract

Titanium dioxide was obtained in its pure form (TiO_2) and in the presence of urea (u-TiO_2) and thiourea (t-TiO_2) using the sol–gel technique. The obtained powders were characterized by BET surface area analysis, Infrared Spectroscopy, Diffuse Reflectance Spectroscopy and the Rietveld refinement of XRD measurements. All the prepared catalysts show high anatase content (>99%). The *a* and *b*-cell parameters of anatase increase in the order TiO_2 < u-TiO_2 < t-TiO_2, while the *c*-parameter presents the opposite trend. Because of the interplay in cell dimensions, the cell grows thicker and shorter when prepared in the presence of urea and thiourea, respectively. The cell volume decreases in the order t-TiO_2 > u-TiO_2 > TiO_2. The photocatalytic activities of the samples were determined on flumequine under solar-simulated irradiation. The most active catalysts were u-TiO_2 and t-TiO_2, reaching values over 90% of flumequine degradation after 15 min irradiation, compared with values of 55% for the pure TiO_2 catalyst. Changing simultaneously the catalyst amount (t-TiO_2) and pH, multivariate analysis using the response surface methodology was used to determine the roughly optimal conditions for flumequine degradation. The optimized conditions found were pH below 7 and a catalyst amount of 1.6 g L^{-1}.

Keywords: Antibiotic; Flumequine; Photocatalysis; Sol–gel; Doped titanium dioxide

1. Introduction

Antibiotics have been designed to reduce diseases, positively impacting on the quality of life and saving many human lives since their introduction. However, when antibiotics are released into the environment with little control, they can become a tremendous problem due to their side effects on natural biota and the development of new resistant bacteria that could result in severe consequences to public health. Antibiotics cannot be naturally degraded and conventional secondary effluent treatments cannot be considered, limiting the possibilities to eliminate them from the environment.

Advanced Oxidation Processes (AOPs) have been proposed as a valuable method to degrade refractory organic compounds due to the uniqueness of hydroxyl radicals to drive organic matter oxidation rendering high reaction rates and low selectivity. Among the AOPs, the photocatalytic method is currently mentioned as one of the most studied technologies. The process presents recognized advantages, such as the low price and chemical stability of the more used catalyst (TiO_2) and the possibility to combine the process with biological decontamination methods [1]. The possibility of using solar light to produce low molecular weight and biodegradable compounds has been mentioned [2]. Among the drawbacks of photocatalysis for industrial applications commonly mentioned are the design of adequate reactors for efficient utilization of photons, catalyst immobilization to avoid the filtration step, and the low absorption of light in the visible region.

The large band gap of TiO_2 (3.2 eV) is the main hindrance to a better utilization of the small UV fraction of the solar light (2–3%). To extend the catalysts' visible light absorption, Ohno et al. [3–6] recently suggested the modification of titania by doping the catalyst with non-metallic atoms, such as nitrogen and sulphur. They suggested that sulphur could be incorporated as a

* Corresponding author. Tel.: +56 41 204600; fax: +56 41 245974.
E-mail address: hmansill@udec.cl (H.D. Mansilla).

0304-3894/$ – see front matter © 2007 Elsevier B.V. All rights reserved.
doi:10.1016/j.jhazmat.2007.11.026

cation replacing Ti ions in the TiO_2 structure. It has also been reported that the photocatalytic activity of TiO_2 in the visible region could be enhanced by nitrogen doped into the TiO_2 lattice [7]. On the other hand, Umebayashi et al. [8] have recently synthesized S-doped TiO_2 with good performance in the visible-light region for methylene blue degradation. They suggest that sulphur anions replace the oxygen atom in the TiO_2 lattice.

The aim of this paper is to determine the photocatalytic activity on the degradation of flumequine while irradiated with simulated solar light of two TiO_2 samples obtained by sol–gel technique in the presence of urea and thiourea. For comparison, pure TiO_2 was also studied. Flumequine, a quinolone structure, is a broad spectrum antibiotic widely used in salmon farms. The obtained data are correlated with the catalysts' structural parameters such as cell size and band gap determinations.

2. Methods

2.1. Catalyst preparation

The catalysts were prepared by the sol–gel technique according to the methodology proposed by Ohno et al. [6]. An ethanolic solution of titanium tetraisopropoxide (0.35 mol L^{-1}) was stirred during 2 h followed by ethanol evaporation at reduced pressure. The obtained gel was calcinated at 500 °C during 3 h. The doped titania samples were obtained by adding urea or thiourea (1:2 molar ratios) to the ethanolic solution. The catalysts were named u-TiO_2 and t-TiO_2, respectively. The samples were sonicated during 20 min and magnetically stirred for 2 h in water (100 mL per 0.5 g catalyst). Before direct use in catalysis, the solids were centrifuged, washed with 1 L of distilled water, and dried.

2.2. Photocatalytic reactions

The photocatalytic activity of the TiO_2 powders was evaluated by measuring the decomposition rate of the antibiotic flumequine in aqueous solution (20 ppm, SIGMA). The reaction was monitored in a Shimadzu 1603 spectrophotometer by measuring the absorption at 248 nm. To prevent possible interferences by formed intermediates, the reaction was also followed by HPLC analysis using a Merck–Hitachi instrument equipped with a LichroCART 250-4 RP-18 column. Acetonitrile/water/methanol (30/55/15) was used as eluent at 3.5 mL min^{-1}. The same results were obtained by both techniques. Irradiation was performed on 60-mL volume solution in a Pyrex reactor with a Suntest XLS$^+$ (Atlas, USA) using irradiance of 500 W m^{-2}.

2.3. Analytical methods

X-ray diffraction patterns were recorded in a Siemens D5000 diffractometer using a Cu Kα radiation. Generator settings were 40 kV, 30 mA. Divergence scattered and receiving slits were 1 mm, 1 mm and 0.2 mm, respectively. A curved graphite monochromator was used. Data were collected in the 2θ range: 22.0–135.995°, with a scanning step of 0.035° and a counting time of 15 s per point. The step width assured a minimum of about 12 intensity points for the narrower peaks. The data were analyzed using the GSAS system [9]. Starting unit-cell parameters and atomic coordinates for anatase and rutile were taken from the literature [10,11]. Peak profiles were fitted using the Thompson–Cox–Hastings pseudo-Voigt function [12]. Mean coherence paths (MCPs) dimensions were calculated taking into account the instrument broadening function, determined using NIST SRM 660 lanthanum hexaboride (LaB_6) standard.

Diffuse reflectance spectra of the sol–gel powders (TiO_2, u-TiO_2 and t-TiO_2) were recorded in a Shimadzu UVPC 3101 spectrophotometer equipped with an integration sphere. The powder samples were directly placed into a cylindrical sample port holder (3 cm diameter, 1 mm deep).

IR spectra were obtained with a FTIR Nicolet 510 P spectrophotometer, using KBr pellets. The pellet concentration was approximately 1% weight.

The Brunauer–Emmett–Teller (BET) surface area of the powders was determined by nitrogen adsorption in a Micromeritics Gemini 2370 instrument. Approximately 0.2 g of sample were degassed at 350 °C for 3 h prior to nitrogen adsorption measurements. The BET area was determined using the adsorption data in the relative pressure (P/P_o) range of 0.005–0.99.

For multivariate analysis, a response surface methodology (RSM) was used as previously described for photocatalytic processes [13,14]. This model is based on a central composite circumscribed design made of a factorial design and star points. The data was analyzed using the Modde 7.0 software. The variable values were coded and normalized in unitary values, −1 and +1, for TiO_2 amount and pH, ranging between 0.85 and 2.15 g L^{-1}, and 7 and 8.2, respectively. From these ranges, the central point (coded 0) was set and determined in triplicate. The star points were distributed at a distance of $n^{1/2}$ from the central point, where n is the number of variables. The response factor was flumequine degradation after 15 min irradiation. The experimental design with the codified and non-codified values is shown in Table 4.

A second-order function that described the system's behaviour was determined by a multiple regression. The optimized values of the analyzed variables were obtained using the Modde 7.0 software. The statistical validation was performed by an ANOVA test with a 95% of confidence.

3. Results and discussion

The crystalline forms of the three catalysts were determined using X-ray diffraction analysis (Fig. 1), and the data was simulated using the Rietveld method [15]. The reliability factors Rwp, R_B and GofF, which describe the goodness of the fittings, are in the range of 8.03–8.94, 1.99–3.67 and 1.11–1.26, respectively (Table 1) and are considered satisfactory.

A comparison of the XRD patterns shows that the peak positions are nearly the same for all the catalysts. The diagrams correspond to anatase phase. Rutile phase was not observed in the samples.

The doped sample, t-TiO_2, shows broader peaks than those of pure and u-doped TiO_2 (Fig. 1, inset). Ohno et al. found

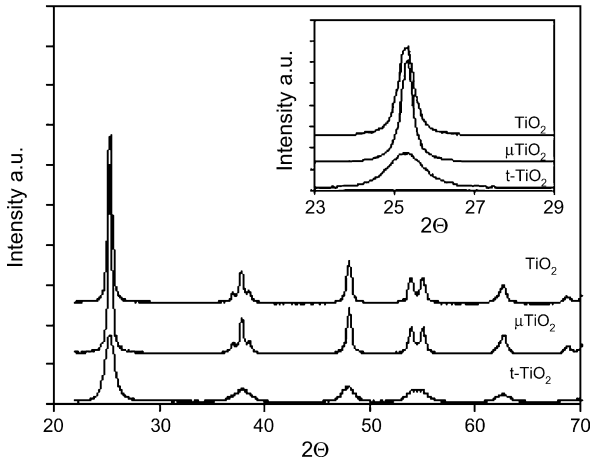

Fig. 1. XRD profiles of synthesized catalysts: pure TiO_2; u-TiO_2 and t-TiO_2. Inset: amplification of the more intense anatase peak of powders.

Table 1
Reliability factors obtained in the Rietveld simulation

Sample	Rwp	Rp	RBragg	GofF
u-TiO_2	8.03	5.64	1.99	1.11
TiO_2	8.27	5.92	2.65	1.15
t-TiO_2	8.94	6.76	3,67	1.26

Rp : $100\sum|I_o - I_c| / \sum I_o$, Rwp : $100\left[\sum w_i(I_o - I_c)^2 / \sum w_i {I_o}^2\right]^{0.5}$, R_B : $100\sum|I_{ko} - I_{kc}| / \sum I_{ko}$, GofF : $\sum w_i(I_o - I_c)^2/(N - P)$. I_o and I_c: observed and calculated intensities, w_i: weight assigned to each step intensity, I_{ko} and I_{kc}: observed and calculated intensities for Bragg k-reflection, N and P: number of data points in the pattern and number of parameters refined.

the same result, suggesting that this catalyst's crystal lattice is locally distorted by the incorporation of ionic sulphur into TiO_2 [4]. In our case, as we did not detect sulphur, the distortions could be probably due to the very low size of the crystallites (see Table 2).

Lattice parameters, phase composition and MCP values for anatase in the samples u-TiO_2 and t-TiO_2, as obtained by the simulation, are shown in the Table 2. Pure TiO_2 parameters are also shown for comparison. TiO_2 and u-TiO_2 contain exclusively anatase; t-TiO_2 predominantly contains anatase (99.42%) and a very small amount of brookite (0.58%). The a- and b-parameters increase in the series, while the c-parameter presents an opposite trend. Accordingly, the cell grows thicker and shorter with the incorporation of urea and thiourea, and the unit cell volume decreases.

The crystallographic information shows that the unit cell is reduced in size when doped with urea and thiourea, which is indicative of the possible atomic substitution into the crystal lattice. These results are consistent with those reported by Ohno et al. [5]. The decrease in unit cell volume may also be attributed to the presence of vacancy sites.

The size of the mean coherence paths, also called crystallite size, shows variations and isotropic dimensions. The addition of urea significantly increases the MCP dimensions, while the addition of thiourea produces the opposite effect.

Compared with pure TiO_2, u-TiO_2 and t-TiO_2 present an intense yellow colouration that remains stable even after sonication and vigorous washing. The diffuse reflectance spectra for each powder are shown in Fig. 2a. A strong absorption in the visible region ($\lambda > 400$ nm) was observed in the samples u-TiO_2 and t-TiO_2. The band was not observed in pure titania. Clearly, u-TiO_2 shows slightly high photoabsorption than t-TiO_2 and is larger than titania. Ohno et al. found that the yellowing of the powder for t-TiO_2 is a function of the calcination temperature [3]. In our preparations, all the samples were obtained under the same calcination conditions (500 °C, 3 h).

Using the reflectance values (R%) and applying the modified Kubelka–Munk function, the powders' band gap were determined from the plot $[F(R)E]^{1/2}$ *vs* the energy of the absorbed light, E, according to Sakthivel et al. [16] (Fig. 2b). This approach gives the values 3.18, 3.15 and 3.16 eV for TiO_2, u-TiO_2 and t-TiO_2, respectively. These values are comparable to those reported by Sakthivel and Kisch for carbon-doped TiO_2 [17]. Although, the values reported here are different from the values found for tiourea-doped TiO_2 [16], the trend to decrease the band gap is related. The shift of the light absorption profile in doped titania has been associated to the presence of manifold surface states close to the valence band edge [16].

To determine the presence of N and/or S in the crystalline framework, infrared analyses were performed. Fig. 3A shows the IR spectrum for pure TiO_2, while Fig. 3B and C shows the spectra for u-TiO_2 and t-TiO_2, respectively.

Clearly, the IR spectra of the doped samples differ notably from the IR spectrum of pure TiO_2 in the range 1800–900 cm^{-1}. Pure TiO_2 does not display any absorption bands in the range. The bands observed at 1410 and 1160 cm^{-1} in Fig. 3B correspond to N=O and N–O stretching, respectively. These values are typical of monodentate nitrite coordinated with a metallic centre [18,19]. The feature band centred at 1050 cm^{-1} and the shoulder at 1330 cm^{-1}, typically correspond to hyponitrite. These results indicate that doping with urea introduces N in the form of nitrite and hyponitrite. Interestingly, the thiourea-doped TiO_2 sample displays an IR spectrum similar to the spectrum of the urea-doped TiO_2. Sulphur-containing species (like sulphates) were

Table 2
Lattice parameters for samples TiO_2, u-TiO_2 and t-TiO_2

Sample	a and b parameters	c parameter	Volume [Å]^3	Phases (wt.%)	Size[a] [Å]	Size[b] [Å]
TiO_2	3.7862 (1)	9.5081 (3)	136.398 (7)	Anatase: 100%	30.01	28.55
u-TiO_2	3.7870 (1)	9.5057 (4)	136.324 (10)	Anatase: 100%	75.66	77.32
t-TiO_2	3.7886 (4)	9.4830 (13)	136.113 (34)	Anatase: 99.42%, brookite: 0.58%	12.62	12.07

Numbers in parentheses indicate the uncertainty in the last significant figure.
[a] Perpendicular.
[b] Parallel.

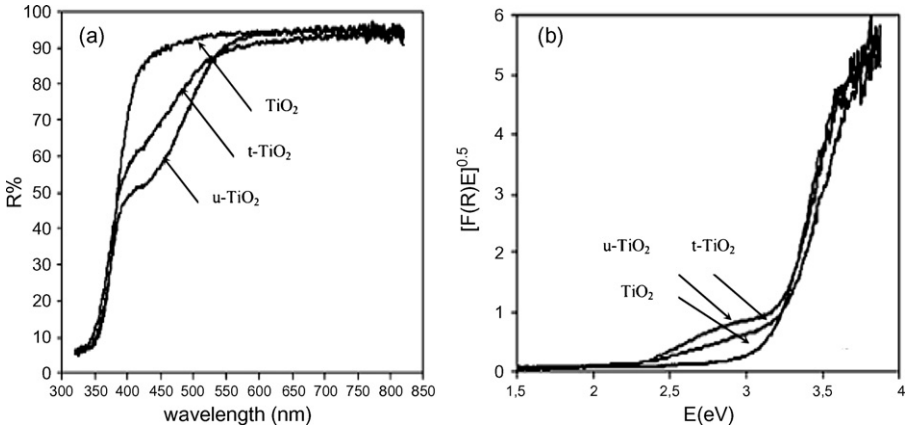

Fig. 2. Diffuse reflectance spectra of pure TiO_2, u-TiO_2 and t-TiO_2 (a); Kubelka–Munk function of the catalyst powders (b).

not detected. In agreement with previous results reported by Sakthivel et al., these results indicate that the products obtained by both techniques are similar in composition, although, the amount of nitrogen in the thiourea-doped sample seems to be lower than in the urea-doped sample [16]. By comparing the plots presented in Fig. 2a with the FTIR spectra, it is clear that colour intensity is related to the amount of dopant. The Sample u-TiO_2 has a strong absorption feature in the range 400–500 nm and a higher amount of dopant, as detected by FTIR.

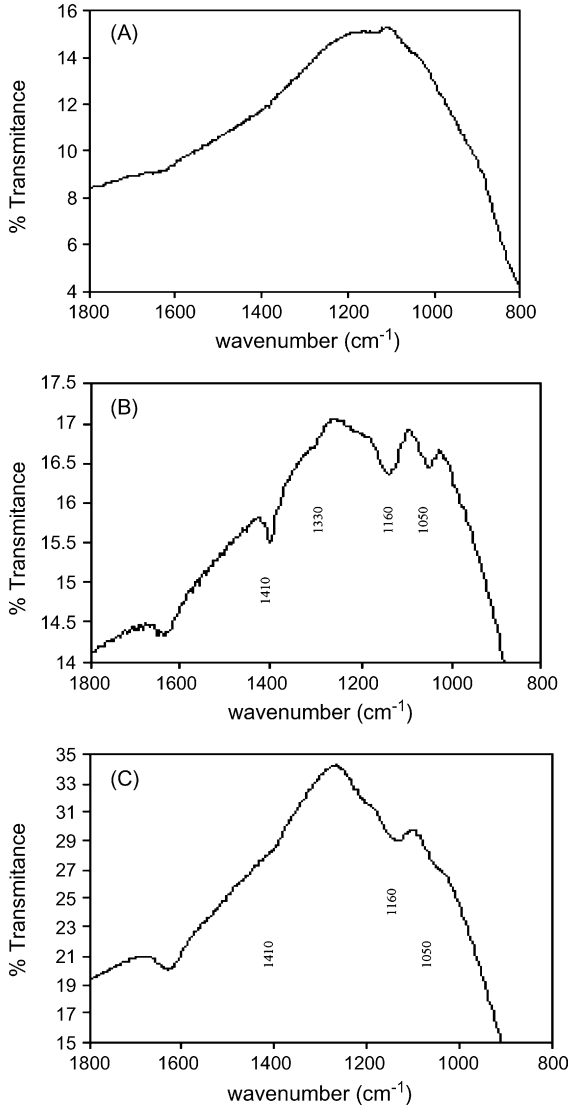

Fig. 3. FT-IR spectrum of TiO_2 (A), u-TiO_2 (B) and t-TiO_2 (C).

Table 3
BET surface and pore volume of the catalysts prepared by sol–gel

Catalyst	S_{BET} (m^2/g)	V_o (cc/g)	V_m (cc/g)
t-TiO_2	71	0.033	0.059
u-TiO_2	50	0.023	0.061
TiO_2	8	0.004	0.009

Table 3 presents the surface areas of the catalysts determined by nitrogen adsorption and BET analysis. The t-TiO_2 and u-TiO_2 powders present higher surfaces compared to pure TiO_2. The micropore volumes (V_0) of doped TiO_2 are several times higher than the pure TiO_2. The mesopore volumes (V_m) also present the same trend, indicating the low porosity of pure TiO_2.

To evaluate the photocatalytic activity of the doped titania samples, the destruction of flumequine was studied. Multivariate analysis and RSM were used to identify optimal reaction conditions. From the results of the factorial planning experiments, shown in Table 4, a polynomial response to flumequine degradation was obtained for the variables pH and amount of t-TiO_2 (Eq. (1)). The polynomial considers the relative importance

Table 4
Calculated and experimental results to flumequine degradation

pH	TiO_2 (g)	Y_{exp} (%)	Y_{calc} (%)
7.01 (−1)	0.85 (−1)	84.2	81.7
8.21 (+1)	0.85 (−1)	66.3	64.8
7.01 (−1)	2.15 (+1)	89.8	89.0
8.21 (+1)	2.15 (+1)	88.6	89.0
6.76 (−1.41)	1.50 (0)	88.9	93.3
8.46 (+1.41)	1.50 (0)	78.4	81.2
7.61 (0)	0.58 (−1.41)	61.5	63.8
7.61 (0)	2.41 (+1.41)	86.1	86.0
7.61 (0)	1.50 (0)	89.4	87.3
7.61 (0)	1.50 (0)	89.4	87.3
7.61 (0)	1.50 (0)	88.0	87.3

Numbers in parentheses represent the coded values used in calculations.

and interactions between the different variables. The coefficients were normalized according to codified variable values. $Y(\%)$ represents the percentage of flumequine degradation after 15 min irradiation considering 95% confidence level for coefficients. The relative significance and interactions between the two variables under study are presented.

$$Y(\%) = 8.76(\pm 0.30) - 0.427\ (\pm 0.254)(\mathrm{pH}) + 0.786(\pm 0.254)(\mathrm{TiO_2}) - 0.619\ (\pm 0.289)(\mathrm{TiO_2})^2 + 0.422\ (\pm 0.360)(\mathrm{pH\,TiO_2}) \quad (1)$$

Considering the first-order effect and the interaction coefficient of each variable, it can be concluded that the main effect is attributable to the TiO_2 amount and that the synergy with the pH is less significant. Antagonistic effect between the variables was not observed. The model was validated through ANOVA test with 95% confidence level. Experimental and calculated data are shown in Table 4. An excellent correspondence between both values that presents an average variation coefficient less than 2% validating the polynomial can be seen.

A 3-D representation of the polynomial is shown in the Fig. 4. It can be seen that the highest FQ degradation is obtained at pH close to 7, in the studied domain, and the amount of catalyst (t-TiO_2) ranging from 1.5 to 1.9 g/L.

The adsorption process performed in the dark during 30 min indicates that t-TiO_2 absorbs around 73% of the initial flumequine concentration (20 ppm), which is a very high value in comparison with 58% and 19% adsorption for u-TiO_2 and pure TiO_2, respectively. After adsorption equilibrium, flumequine initial concentrations in the solution were 5.4, 8.4 and 16.2 ppm for t-TiO_2, u-TiO_2 and TiO_2, respectively. Under illumination with simulated solar light it decayed exponentially with apparent first-order constant ($R^2 \sim 0.999$) of 0.08, 0.07 and 0.03 min^{-1} for u-TiO_2, t-TiO_2 and TiO_2, respectively.

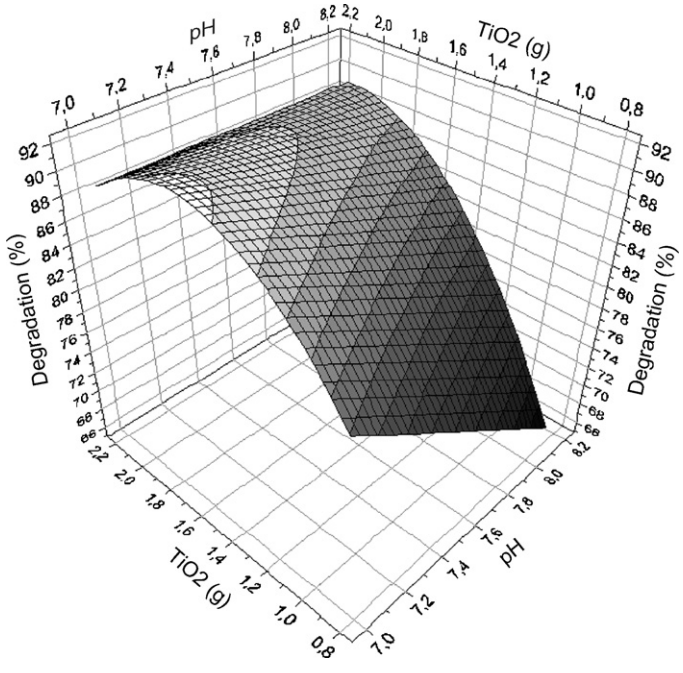

Fig. 4. Response surface for multivariate analysis of flumequine photocatalysis using t-TiO_2 catalyst.

The difference in adsorption could be associated with the differences in surface area and pore volumes: the higher the surface area and pore volumes, the higher is the amount of flumequine adsorbed by the photocatalysts in the dark. The dopant exerts an important influence on the photocatalyst's microstructure, resulting in materials with high surface area and adsorbent capacity. In the case of t-TiO_2, the dopant's effect seems to be related to the obstruction of crystallite growth. This effect was reported previously for other dopants [20,21]. On the other hand, in the case of u-TiO_2, crystallite sizes are even bigger than in pure TiO_2, which means that another unknown mechanism is involved in the control of surface area for this type of samples. The microscopic structure of t-TiO_2 was also analyzed using SEM micrograph (data not shown), which indicated a fine, agglomerated powder. The catalyst's surface appears rough, an aspect that could enhance the catalyst's surface area and adsorption properties.

The significant effect of u-TiO_2 and t-TiO_2 in the elimination of flumequine from water is principally due to the adsorption phenomena. However, the photocatalytic activity of doped titania is also observed to be similar and higher than the observed for pure TiO_2 (photolysis is negligible in absence of catalyst). The small change in the band gap observed in doped titania could somewhat improve the absorption of visible light, but it is not necessarily the main cause of the increment of their photocatalytic activity. Sakthivel and Kisch [17] propose that the photocatalytic activity of these materials under visible light is consequence of the production of superoxide radicals ($O_2^{\bullet -}$) by reduction of adsorbed O_2. The absorption of light promotes electrons from surface states located close to the valence band edge to the conduction band. Since the redox potential of the trapped electrons is c.a. −0.64 [16] the adsorbed O_2 can be reduced to $O_2^{\bullet -}$, which is a moderate oxidant that can trigger the oxidation of flumequine. In our case the absorption of light begins at 520 nm (2.38 eV) while the band gap energy is c.a. 3.18 eV; this result suggests the presence of surface states close to the valence band as was previously reported [16,17].

4. Conclusion

Doped catalysts were successfully prepared by sol–gel methodology. Their crystalline structure was determined by XRD analysis. A diminution of the cell unit was observed in samples doped with urea and thiourea compared with that of pure titania. This fact has been attributed to the incorporation of nonmetals in the oxide lattice. The presence of nitrogen as nitrite and hyponitrite were determined by FT-IR. The high adsorption found for t-TiO_2 and u-TiO_2 correlates well with the BET surface area. Doped titania presents a higher catalytic activity in the visible region in comparison with pure titania, related with reduction of adsorbed O_2 by electrons promoted from surface states to the conduction band.

Acknowledgement

This work was supported by the Fondo Nacional de Ciencia y Tecnolgía (FONDECYT, Chile) grant 1040460 and by CONICET PIP 5215, ANPCyT PICT 33973 (Argentina).

References

[1] M. Hoffmann, S. Martin, W. Choi, D. Bahnemann, Chem. Rev. 95 (1995) 69–96.
[2] J.-M. Herrmann, Top. Catal. 34 (2005) 49–65.
[3] T. Ohno, T. Mitsui, M. Matsumura, Chem. Lett. 32 (2003) 364–365.
[4] T. Ohno, T. Tsubota, K. Nishijima, Z. Miyamoto, Chem. Lett. 33 (2004) 750–751.
[5] T. Ohno, M. Akiyoshi, T. Umebayashi, K. Asai, T. Mitsui, M. Matsumura, Appl. Catal. A 265 (2004) 115–121.
[6] T. Ohno, Water Sci. Technol. 49 (2004) 159–163.
[7] R. Asahi, T. Morikawa, T. Ohwaki, A. Aoki, Y. Taga, Science 293 (2001) 269–271.
[8] T. Umebayashi, T. Yamaki, S. Yamamoto, A. Miyashita, S. Tanala, T. Sumita, K. Asai, J. Appl. Phys. 93 (2003) 5156–5160.
[9] A.C. Larson, R.B. Von Dreele, Report LAUR 86-748, Los Alamos National Laboratory, 1994.
[10] J.K. Burdett, T. Hughbanks, C.J. Miller, J.W. Richardson, J.V. Smith, J. Am. Chem. Soc. 198 (1987) 3539–3646.
[11] E.P. Meagher, G.A. Lager, Can. Mineral. 17 (1979) 77–84.
[12] P. Thompson, D.E. Cox, J.B. Hastings, J. Appl. Crystallogr. 20 (1987) 79–83.
[13] C. Lizama, J. Freer, J. Baeza, H.D. Mansilla, Catal. Today 76 (2002) 235–246.
[14] J. Fernandez, J. Kiwi, C. Lizama, J. Freer, J. Baeza, H.D. Mansilla, J. Photochem. Photobiol. A 151 (2002) 213–219.
[15] H.M. Rietveld, J. Appl. Crystallogr. 2 (1969) 65–71.
[16] S. Sakthivel, M. Janczarek, H. Kisch, J. Phys. Chem. B 108 (2004) 19384–19387.
[17] S. Sakthivel, H. Kisch, Angew. Chem. Int. Ed 42 (2003) 4908–4911.
[18] K. Nakamoto, Infrared and Raman Spectra of Inorganic and Coordination Compounds, fourth ed., John Wiley, NY, 1986, Part III, p. 225.
[19] F. Prinetto, G. Ghiotti, I. Nova, L. Lietti, E. Tronconi, P. Forzatti, J. Phys. Chem. B 105 (2001) 12732–12745.
[20] A.M. Ruiz, A. Cornet, J.R. Morante, Sens. Actuators B 100 (2004) 256–260.
[21] J.F. Bandfield, B. Bischoff, M.A. Anderson, Chem. Geol. 110 (1993) 211–231.